Received: 4 September 2017 | Accepted: 13 December 2017
DOI: 10.1002/jbio.201700252

Journal of BIOPHOTONICS

FULL ARTICLE

Aspects of silver tolerance in bacteria: infrared spectral changes and epigenetic clues

Rafig Gurbanov[1,2] | Nihal S. Ozek[3] | Sinem Tunçer[2] | Feride Severcan[2,4*] | Ayse G. Gozen[2]

[1]Department of Molecular Biology and Genetics, Bilecik Şeyh Edebali University, Bilecik, Turkey
[2]Department of Biological Sciences, Middle East Technical University, Ankara, Turkey
[3]Department of Biology, Ataturk University, Erzurum, Turkey
[4]Department of Biophysics, Faculty of Medicine, Altinbas University, Istanbul, Turkey

***Correspondence**
Feride Severcan, Department of Biological Sciences, Middle East Technical University, Ankara 06800, Turkey.
Email: feride@metu.edu.tr

Funding information
Tübitak, Grant/Award number: 113Y515

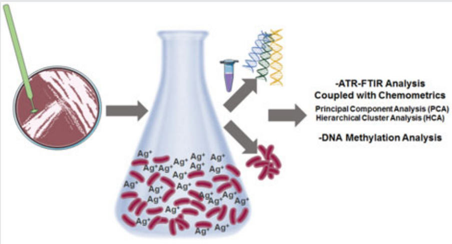

In this study, the molecular profile changes leading to the adaptation of bacteria to survive and grow at inhibitory silver concentration were explored. The profile obtained through infrared (IR)-based measurements indicated extensive changes in all biomolecular components, which were supported by chemometric techniques. The changes in biomolecular profile were prominent, including nucleic acids. The changes in nucleic acid region (1350-950 cm^{-1}) were encountered as a clue for conformational change in DNA. Further analysis of DNA by IR spectroscopy revealed changes in the backbone and sugar conformations. Moreover, Enzyme-Linked Immunosorbent Assay-based measurements of DNA methylation levels were performed to see if epigenetic mechanisms are in operation during bacterial adaptation to this environmental challenge. The results indicated a notable demethylation in *Escherichia coli* and methylation in *Staphylococcus aureus* likely to be associated with their elaborate adaptation process to sustain survival and growth.

KEYWORDS
bacteria, FTIR, methylation, silver

1 | INTRODUCTION

Bacteria adapt themselves to survive and grow in polluted areas [1]. Among polluting metals, silver (Ag) compounds make up a part of industrial wastes and has been shown to be poisonous [2], although mechanisms of its toxicity are still poorly understood [3]. Therefore, it has been considered as serious pollutant [3]. Adaptation of bacteria to heavy metals is common for protection against their deleterious effects by the restriction of the metal uptake or sequestration [4]. In addition, bacteria may detoxify metal ions and convert them to less toxic states [5, 6].

As can be inferred from the existing literature, most of the research has been conducted on the expression of candidate genes. However, the wide-ranging profile of the biomolecular changes leading to the adaptation of bacteria to toxic Ag levels has not been documented yet. For this purpose, the molecular elucidation capacity of infrared (IR) spectroscopy was used in this study. IR spectroscopy is ideal to visualize gross molecular changes and with accompanying chemometric tools the detection of critical and pronounced changes in specific molecules is possible [7]. By using its advantages, global biomolecular alterations in lipids and proteins occurring in cobalt (Co)-acclimated *Escherichia coli*, *Bacillus* sp. and *Pseudomonas* sp. and cadmium (Cd) and lead (Pb)-exposed *E. coli* and *Staphylococcus aureus* were identified in our previous studies [8, 9]. In addition, the spectral changes in nucleic acid structure and content were reported. It was proposed that there might be a link between those changes and DNA methylation. Since it is

https://doi.org/10.1002/jbio.201700252

well documented that environmental stressors may lead to epigenetic modifications including methylation [10]. It is known that the bacteria can develop different adaptive mechanisms for different heavy metals [11, 12]. Therefore, this study was conducted to demonstrate the Ag-driven molecular alterations in lipid, protein and in the backbone structures and sugar puckering modes of DNA in *E. coli* and *S. aureus* using IR spectroscopy. Furthermore, their DNA methylation status was directly measured and by the way, the link between the Ag-driven spectral changes in nucleic acids and DNA methylation was shown, for the first time.

2 | MATERIALS AND METHODS

The details of the experimental section can be found in the Supporting information of this manuscript.

2.1 | Bacterial growth conditions

E. coli ATCC 8739 and *S. aureus* ATCC 6538 strains were grown at 28°C under aerobic conditions, in an orbital shaker (Zhicheng, China) at 200 rpm.

2.2 | Collection of IR spectra and data analysis

The bacterial concentrations were adjusted to 0.5OD in UV-VIS spectrophotometer (UV-2600/2700, Shimadzu, Japan) at 600 nm in 2 mL of total volume.

Spectrum 100 FTIR spectrometer (PerkinElmer, USA) equipped with a Universal ATR accessory was used to collect the IR spectra of bacteria. In data analyses, the second derivative and vector-normalized IR spectra were used.

2.3 | Principal component analysis (PCA) and hierarchical cluster analysis (HCA)

PCA and HCA were applied to second derivative and vector-normalized IR data of the control and Ag-exposed bacteria in the whole IR region (4000-650 cm^{-1}) using Unscrambler X 10.3 (CAMO Software AS., Oslo, Norway) multivariate analysis (MVA) software.

2.4 | DNA methylation assay

The global DNA methylation status of bacteria was detected using MethylFlash Methylated DNA Quantification Kit (Epigentek, USA).

2.5 | Statistical data analysis

The result were expressed as means ± standard error of mean (SEM). Ag-exposed vs control groups were analyzed statistically using Student's *t* test. Pearson's correlation was used to evaluate the association between 2 or more variables. Data analyses and graphing were performed with GraphPad Prism 6.01 (GraphPad Software, Inc., CA, USA.).

3 | RESULTS AND DISCUSSION

In this study, the molecular changes occurring in *E. coli* and *S. aureus* growing at inhibitory Ag concentrations were investigated. Ag inhibitory concentrations were determined as 130 μM for *E. coli* and 94 μM for *S. aureus*. The bacteria were grown in their minimal inhibitory concentration followed by several passages. In our previous work [8], the growth of the same bacteria under inhibitory concentrations of Cd and Pb was evaluated. In that study, Cd inhibitory concentrations were found as 171 μM for *E. coli* and *S. aureus*, while Pb inhibitory concentrations were determined as 226 and 100 μM for *E. coli* and *S. aureus*, respectively. It was deduced that even though these bacteria can grow in the presence of the mentioned heavy metals, it appeared to be less tolerant to Ag and Cd than they were to Pb.

To elucidate Ag adaptation-induced molecular changes, IR spectroscopy was applied since it enables to describe variations in environmentally caused alterations in the organisms through the analysis of vibrational bands of specific molecules [13]. Our previous studies have proved the power of this technique in the detection of structural and functional alterations of biomolecules in bacteria due to Co, Cd and Pb adaptation [8, 9]. Similarly, visual inspection analyses of the control and Ag-exposed *E. coli* and *S. aureus* spectra in the whole IR region (4000-650 cm^{-1}) showed differences between exposed and untreated bacteria (Figure S1A and B in File S1). To identify these alterations in a quantitative manner, the detailed spectral analyses, such as positions and intensities of all bands and bandwidths of some specific bands, were performed at 2980-2830, 1750-1350 and 1350-950 cm^{-1} regions (Figure 1; Table 1). The assignments of analyzed bands are shown in Table S1 in File S1.

To determine the variations in the lipid constituents of control and Ag-exposed bacteria, the spectral bands located at C─H stretching (2980-2830 cm^{-1}) region were analyzed (Figure 1A and B). This region contains several spectral bands arising mostly from lipid functional groups along with small contributions from protein [8, 14]. To define changes of the lipid content due to Ag adaptation, the intensity of the CH_2 antisymmetric band located at 2924 cm^{-1} emerging from antisymmetric stretching vibrations of the functional groups in lipid was measured. As can be seen from Table 1, the intensity of this band increased significantly in the Ag-exposed bacteria evidencing elevated lipid content [15]. The elevated lipid concentrations indicate an alteration in lipid metabolism [9, 16]. On the contrary, we found a decrease in lipid amounts in Cd- and Pb-exposed bacteria in our former study [8]. This different response may be explained with the diverse adaptation ways in microorganisms dealing with different metals. The elevated

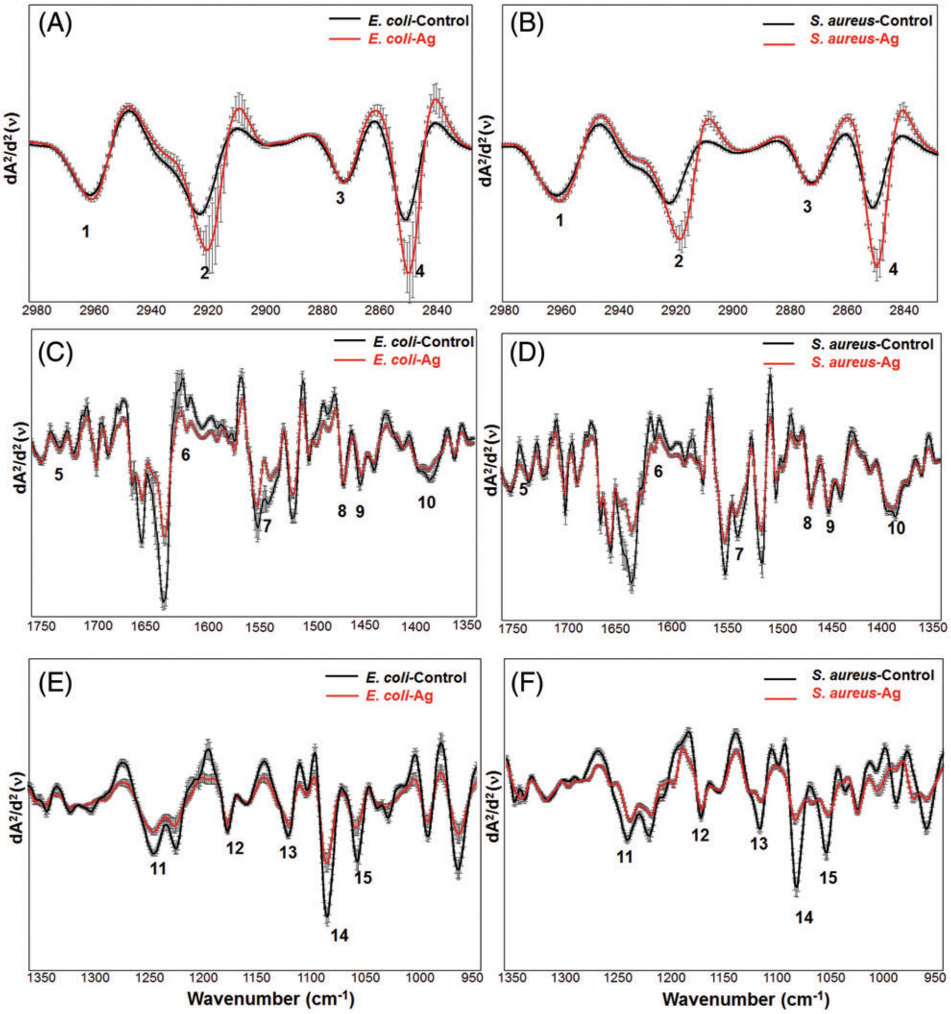

FIGURE 1 The second-derivative average (solid line) and standard deviation (error bar) of IR spectra of the control and Ag-exposed *Escherichia coli* (A, C, E) and *Staphylococcus aureus* (B, D, F) in the (A, B) 2980-2830 cm^{-1}, (C, D) 1750-1350 cm^{-1} and (E, F) 1350-950 cm^{-1} spectral regions, respectively

TABLE 1 Changes in the intensity (%), position and bandwidth values of the IR bands for control and Ag-exposed bacteria

Band name	*Escherichia coli*		*Staphylococcus aureus*	
	Control	**Ag-exposed**	**Control**	**Ag-exposed**
Band absolute intensity (%)				
CH$_2$ antisym. Stretch.-lipid (2924 cm^{-1})	100.0 ± 3.14	109.71 ± 1.93↑**	100.0 ± 0.53	106.88 ± 2.78↑*
Amide I-protein (1635 cm^{-1})	100.0 ± 3.06	86.41 ± 1.77↓****	100.0 ± 6.06	84.45 ± 1.72↓*
PO$_2^-$ antisym. Stretch.-nucleic acids (1238 cm^{-1})	100.0 ± 3.09	92.62 ± 1.45↓***	100.0 ± 2.00	88.63 ± 2.22↓***
C─O stretch.-RNA (1118 cm^{-1})	100.0 ± 3.14	92.44 ± 1.45↓*	100.0 ± 3.31	57.03 ± 1.47↓****
C─O stretch.-polysaccharide (1057 cm^{-1})	100.0 ± 1.91	71.05 ± 5.48↓****	100.00 ± 3.95	60.81 ± 2.20↓****
B-form DNA (936 cm^{-1})	100.0 ± 1.26	30.37 ± 0.01↓***	100.0 ± 1.72	0.0 ± 0.0↓ ***
Main *A*-form marker (1245 cm^{-1})	100.0 ± 1.02	202.40 ± 1.02↑***	100.0 ± 5.0	390.0 ± 5.0↑***
Main *Z*-form marker (1214 cm^{-1})	100.0 ± 0.50	232.32 ± 0.50↑****	100.0 ± 1.28	100.0 ± 1.28
Main *N*-type sugar marker (883 cm^{-1})	100.0 ± 2.32	88.37 ± 0.0↓	100.0 ± 0.84	288.13 ± 15.12↑**
Main *N*-type sugar marker (867 cm^{-1})	100.0 ± 0.04	37.69 ± 0.04↓****	100.0 ± 2.50	550.00 ± 2.50↑****
Main *S*-type sugar (838 cm^{-1})	100.0 ± 0.50	333.33 ± 0.50↑****	100.0 ± 0.31	88.05 ± 0.0↓**
Band position (cm^{-1})				
CH$_2$ antisym. Stretch.-lipid (2924 cm^{-1})	2925.78 ± 0.12	2921.41 ± 0.21↓****	2921.75 ± 0.09	2917.37 ± 0.10↓****
Amide I-protein (1635 cm^{-1})	1638.27 ± 0.33	1639.16 ± 0.23↑*	1639.21 ± 0.13	1640.63 ± 0.28↑****
PO$_2^-$ antisym. Stretch.-nucleic acids (1238 cm^{-1})	1238.00 ± 0.31	1236.00 ± 0.53↓***	1239.00 ± 0.45	1236.00 ± 0.17↓***
Bandwidth (cm^{-1})				
CH$_2$ antisym. Stretch.-lipid (2924 cm^{-1})	13.53 ± 0.319	12.77 ± 0.15↓**	12.68 ± 018	11.77 ± 0.29↓*

Downward arrow indicates a decrease and upward arrow indicates an increase. Error bars or uncertainties in a reported measurement are presented as means ± standard error of the mean (SEM). The degree of significance was denoted as less than or equal to $*P \le .05$, $**P \le .01$, $***P \le .001$ and $****P \le .0001$

lipid content under Ag exposure could arise from the well-documented phenomena of intracellular lipid vesicle formation [17, 18].

Ag-adaptation-induced alterations in membrane lipid dynamics and order were evaluated by calculating the bandwidth and position of the CH_2 antisymmetric stretching mode, respectively. The bandwidths of the CH_2 antisymmetric stretching modes were significantly narrowed (Table 1), while its positions shifted significantly to lower values in the Ag-exposed bacteria (Table 1). The decreased bandwidths indicate that the lipids were less mobile. The shift of the position of the same band to lower values implies increased lipid order, which is a marker of membrane rigidity [9].

The changes in the polysaccharides under Ag adaptation were evaluated by calculating the intensity of C—O stretching band located at 1057 cm^{-1} [8]. A significant decrease in the band intensities for this band was measured in the Ag-exposed bacteria (Table 1), indicating diminished polysaccharide content [8], in accordance with our previous findings on Co-acclimated bacteria [9]. On the other hand, these results are opposed to those obtained from Pb exposure [8]. It is well known that polysaccharides are sugar polymers in the cell walls of bacteria and found as extracellular polysaccharides (EPSs) [19]. Moreover, EPSs are secreted out of the cell to cope with environmental stressors including metals [20] and anionic character of these sugars enable them to bind the metal cations efficiently and prevent entry. The primary role of EPS in Gram-negative bacteria's adaptation to Pb has been reported [21]. Therefore, the differences in the polysaccharides content of Pb and Ag-exposed bacteria may indicate that Ag adaptation does not require elevated EPS synthesis.

To determine the changes in the amount and structure of the proteins of Ag-exposed bacteria, the intensities and positions of amide I band located at 1635 cm^{-1} emerging from proteins were evaluated [22]. The IR spectra of control and Ag-exposed bacteria including this band in the 1750-1350 cm^{-1} region are shown in Figure 1C and D. Moreover, the intensities and positions of this band are presented in Table 1. The significant decrease in the intensities of amide I band (Table 1) evidenced a decrease in protein concentrations [9]. The shift in the positions of amide I band to higher values in the Ag-exposed bacteria (Table 1) demonstrated the structural alterations in proteins [15]. The decreased protein content in Cd- and Pb-exposed bacteria that we measured in our previous study is in agreement with the results of this study [8].

To gather information about nucleic acids, the intensities and positions of the PO_2 antisymmetric band located at 1238 cm^{-1} and intensity of the C—O stretching band located at 1118 cm^{-1} were measured. The IR spectra containing these bands in 1350-950 cm^{-1} spectral region are shown in Figure 1E and F. The comparison of the intensities of the PO_2^- antisymmetric stretching band is given in Table 1 for 2 bacteria. The significant decrease in the intensities of this band for the Ag-exposed bacteria indicates a decreased nucleic acid concentration [8]. Moreover, the position of this band significantly shifted to lower values for Ag-exposed bacteria (Table 1), which displays structural alterations in nucleic acids [9]. The comparison of the intensities of the band due to the C—O stretching of RNA revealed a significant decrease in both Ag-exposed bacteria (Table 1), demonstrating decreased RNA content [9] and supporting our former study dealing with Cd- and Pb-exposed bacteria [8].

Ag-adaptation-induced changes in DNA conformational forms were analyzed from isolated bacterial DNA. The intensities (%) of *B*-forms of DNA decreased in *E. coli* and even disappeared in *S. aureus* (Table 1). However, the intensities of main *A*-forms increased in DNA's of both bacteria (Table 1). Main *Z*-form signals also intensified in *E. coli* DNA, but did not seem to change in *S. aureus* (Table 1).

The changes in DNA sugar puckering between the control and Ag-exposed groups were also examined. The intensities (%) of main *N*-type sugars decreased in Ag-exposed *E. coli,* while they increased in Ag-exposed *S. aureus.* However, the intensities (%) of main *S*-type sugars exhibited the reverse trend (Table 1). In other words, *S*-type sugar puckering modes were prevalent in DNA of Ag-exposed *E. coli*, while *N*-type sugar puckering modes were predominant in DNA of Ag-exposed *S. aureus.* Together with this fact, the changes in DNA IR signals canalized us to look for epigenetic motifs, since they create a further transcriptional regulation that supervise gene expression [2, 10]. The comparison of the quantities (%) of 5-methylcytosine (5-*m*C) for the control and Ag-exposed bacteria are shown in Figure 2 as fold changes. A significant 34% decrease was found in the methylated DNA amount in Ag-exposed *E. coli.* On the other hand, Ag-exposed *S. aureus* showed a significant 40% increase in DNA methylation. 5-*m*C level was found as

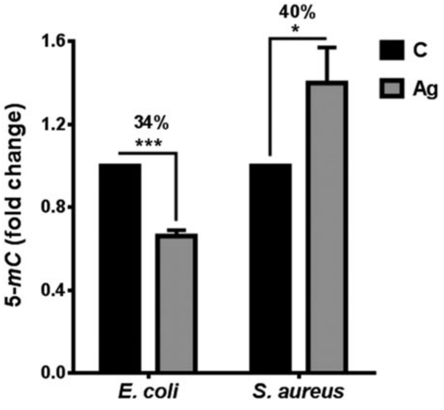

FIGURE 2 Fold changes of the quantity (%) of 5-methylcytosine (5-*m*C) for control and Ag-exposed *Escherichia coli* and *Staphylococcus aureus*. Error bars or uncertainties in a reported measurement are presented as means ± standard error of the mean. The degree of significance was denoted as *$P \leq .05$ and ***$P \leq .001$

0.84% for control *E. coli*, which is consistent with the literature [23]. Obviously, both bacteria behave differently under Ag exposure. The basis of the different epigenetic response in *Staphylococcus* can be due to its basal, endogenous methylation level and sequence properties since the 5-*m*C level of control *S. aureus* was found to be inherently less than that of *E. coli* (0.3% and 0.84%, respectively).

Finally, to support all IR spectral findings, chemometric techniques (PCA and HCA) were also applied. Accordingly, PCA was implemented since loadings and score plots of this analysis enable to determine which variables stand for the foremost dissimilarity. Loadings plots, given in Figure 3A and B, pointed out remarkable differences between control and Ag-exposed bacteria. These differences were prominent in the 3050-2800 cm^{-1} and 1800-690 cm^{-1} regions, corresponding to lipid and fingerprint regions, respectively. High Eigen vector values indicated the presence of measurable variations in the biomolecular profile of bacteria. Score plots demonstrated in Figure 4A and B showed a clear-cut segregation of Ag-exposed samples from the controls. As shown in the figures, the maximum variation values were notable (*E. coli* PC1 + PC2 = 88% and *S. aureus* PC1 + PC2 = 82%).

HCA was applied for the discrimination purpose as a second chemometric tool. The dendrograms presented in Figure 5A and B, confirmed that the Ag-exposed and control bacteria were totally differentiated from each other (15/15) at the maximum distance values [24, 25]. Both chemometrics confirmed the large differences between control and Ag-exposed bacteria.

Bringing together all the gathered information, Ag was found to induce wide-ranging/gross changes in cellular biomolecules in both Gram-negative *E. coli* and Gram-positive *S. aureus* model systems used in this study. Although heavy-metal cations are important as trace elements in biochemical reactions, at higher concentrations they lead to toxic effects. Under metal-stressed conditions, bacteria evolve various strategies and develop tolerance to survive [26]. Since such metal-tolerant microorganisms have the potential to be used as successful bioremediation agents,

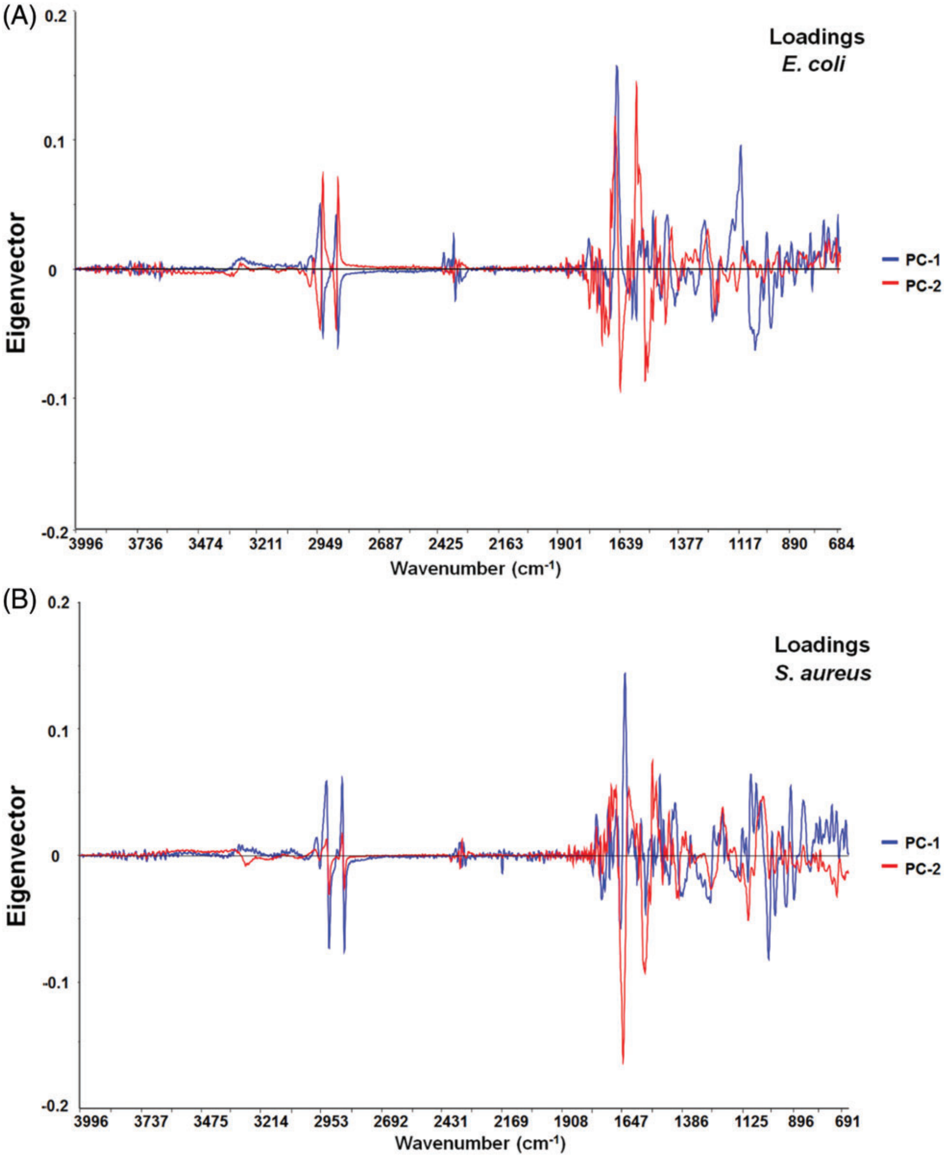

FIGURE 3 PCA loadings plots for the control and Ag-exposed *E. coli* (A) and *S. aureus* (B) in the 4000-650 cm^{-1} spectral region

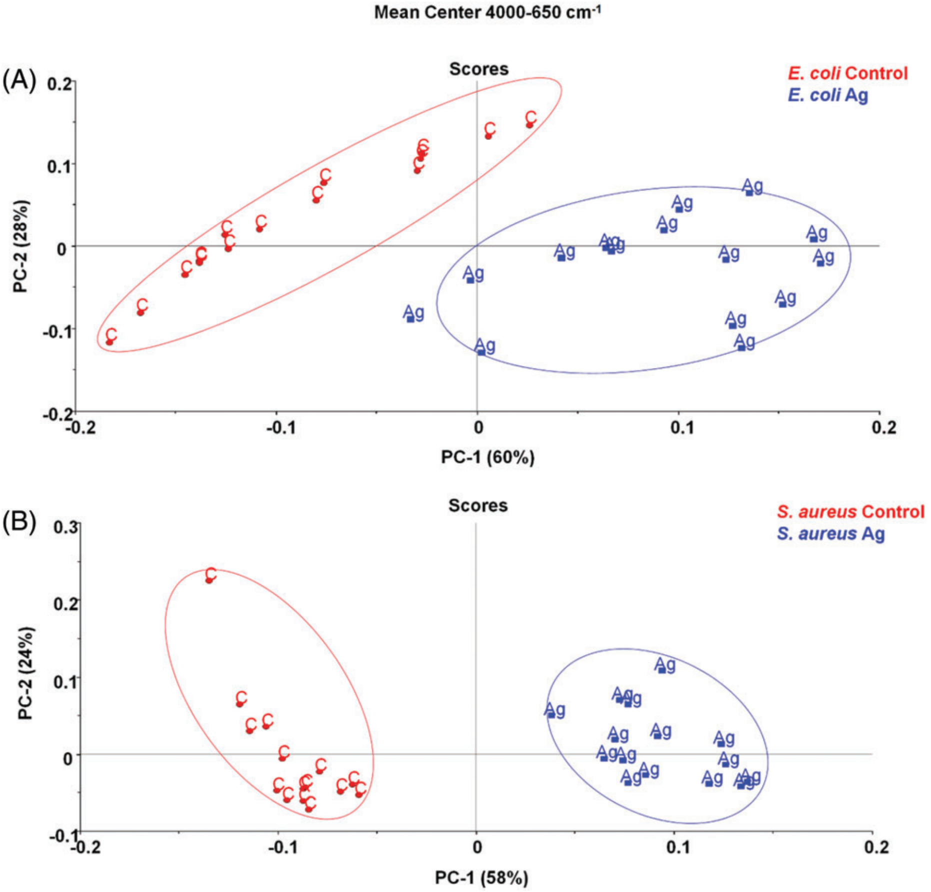

FIGURE 4 PCA score plots for the control and Ag-exposed *Escherichia coli* (A) and *Staphylocccus aureus* (B) in the 4000-650 cm^{-1} spectral region

understanding the physiology of metal-tolerant bacteria is fundamental.

In both bacteria, Ag exposure was found to increase cellular lipid content while decreasing membrane fluidity. These results suggest a possible mechanism that upregulated lipid biosynthesis, thus decreasing membrane fluidity, which is known to be associated with decreased membrane permeability [27, 28]. Environmental stress has also been shown to alter the saturation/unsaturation, cis/trans and branched/unbranched structures of lipids as well as to change membrane bilayer thickness, stability and fluidity [29, 30]. Diminished polysaccharide content in both Ag-exposed bacteria further supports the argument that the tolerance involves the generation of mechanisms for the protection of cell membrane and cellular integrity against heavy-metal-induced damage.

Together with lipids, cellular protein content was also found to be affected by Ag exposure, which is decreased in both *E. coli* and *S. aureus*. Decreased protein synthesis is shown to be consistent with decreased DNA and RNA content in Ag-exposed bacteria with respect to the control, since Ag is known to inhibit DNA replication, transcription and translation processes [31]. Moreover, structural alterations in protein structures were observed in Ag-exposed *E. coli* and *S. aureus*. Being a metal cation, Ag tends to bind to thiol groups of proteins and also can interact with physiological ions and change the protein structure [11, 32]. Consequently, ribosomes may also be denatured as well as translation and transcription can be blocked [31]. *E. coli* is known to divide in every 20 minutes under optimal conditions, while its DNA replication is terminated in 40 minutes. Therefore, under optimal conditions there are many partial copies of the DNA molecules in progressing lateral forks [33], generating high DNA content. A lower DNA content in the presence of Ag was measured as an indication for hindered DNA synthesis. This result is expected since the applied dose of Ag has growth inhibitory effect. Similarly, Feng et al stated that DNA converted from the relaxed state to the condensed state in Ag-treated bacteria, correlated with the decrease in replication [32]. Moreover, our data pointed out a decrease in RNA content indicating slowed down transcriptional activities, which may result in diminished protein levels.

In addition to the decrease in nucleic acid content, we found that Ag alters nucleic acid structure, which may be caused by the capacity of Ag to bind nucleic acids, directly [34]. Furthermore, it can cause DNA damage by the generation of reactive oxygen species [35, 36]. These effects may result in changes in the degree of DNA supercoiling which is highly responsive to environmental conditions [37]. Our results also suggest that Ag exposure can change DNA architecture by altering DNA topology besides conformation of sugar moieties. We found that Ag exposure caused a major reduction of *B*-DNA in favor of *A*-DNA. As previously reported, *B* to *A*-form transitions in DNA are often associated with environmental stress [38]. Additionally, Ag exposure in *E. coli* was found to induce *Z*-DNA formation while we did not observe any change in *Z*-DNA amount in *S. aureus*. The binding of metals to nucleotides does influence the sugar conformation, thus affects the orientation of DNA bases with respect to the axis of helix. In *B*-DNA, all sugars are in C2′-endo puckering (*S*-type conformation), in *A*-DNA all sugars are in C3′-endo puckering (*N*-type conformation) [39]. In *S. aureus*, *N*-type conformation was found to be enhanced by Ag exposure, in accordance with the increase in *A*-DNA. On the other hand, Ag exposure favored *S*-type conformation over *N*-type conformation in *E. coli*, indicating the conversion from *N*-type to *S*-type conformation, caused by increased *Z*-DNA conformation which adopts a C2′-endo puckering [40]. It is worthy of note that in *S. aureus*, Ag did not enhance Z-type structure which is known to be formed by specific DNA sequence motifs with alternating pyrimidines and purines, preferably (CG)n [41].

Finally, we investigated the alterations in DNA methylation pattern in Ag-exposed bacteria. Although the impact of epigenetics on heavy-metal-induced alterations of gene expression is a well-known phenomenon in eukaryotes [42], to the best of our knowledge, the relationship between the heavy-metal adaptation and epigenetic mechanisms has not been investigated in bacteria. On the other hand, increasing number of studies highlights the significance of DNA cytosine methylation in bacteria and emphasize that DNA methylation may have physiological roles including regulation of gene expression. In *Helicobacter pylori*, deletion of an orphan C5-cytosine methyltransferase alters the expression of genes involved in motility, adhesion and virulence [43]. DNA cytosine methyltransferase knockout *E. coli* were found to overexpress the drug resistance transporter SugE [23]. In another study, lack of DNA cytosine methylation has been shown to increase expression of the stress response

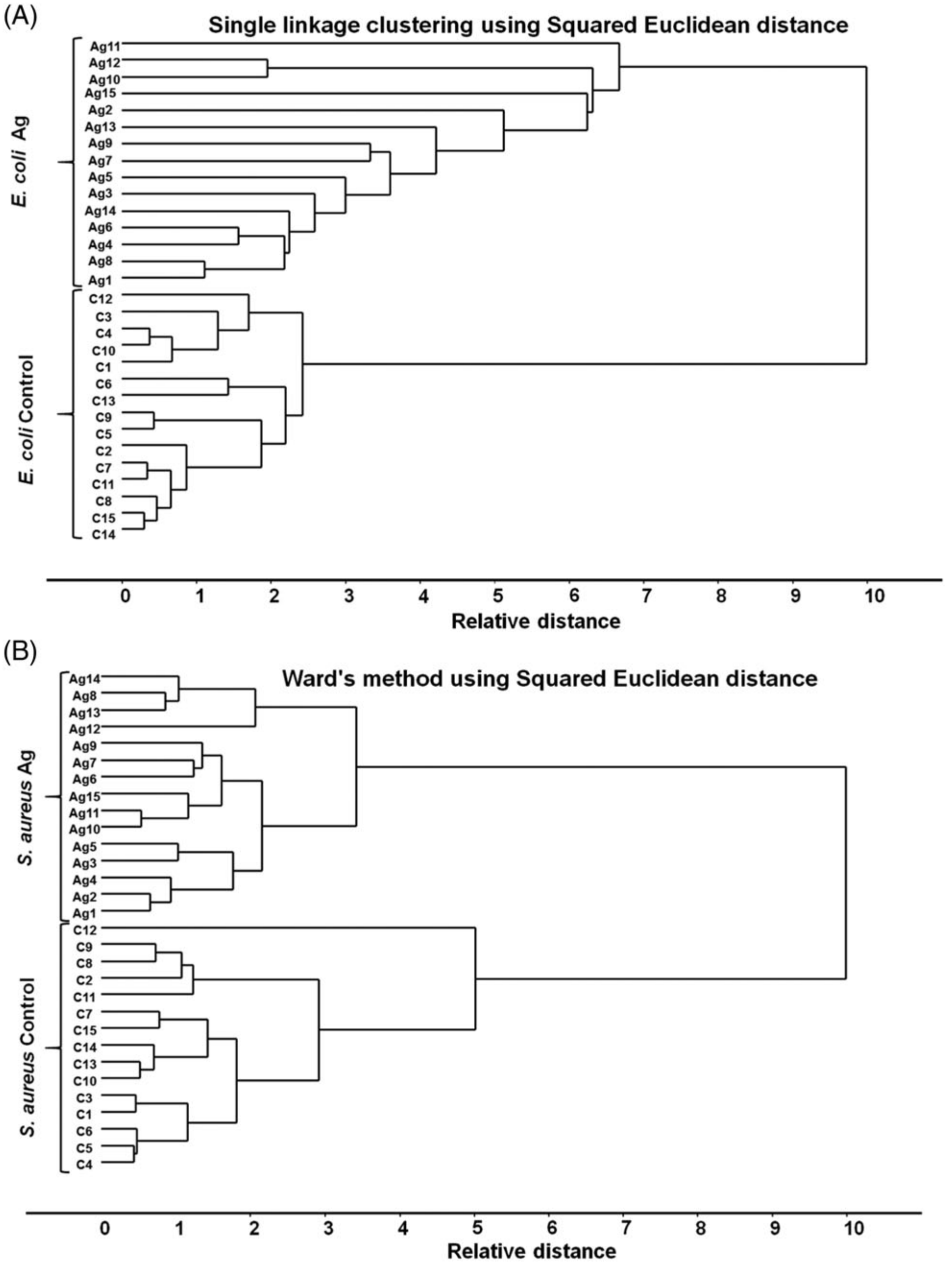

FIGURE 5 Hierarchical cluster analysis of the control and Ag-exposed *E. coli* (a) and *S. aureus* (B) in the 4000-650 cm^{-1} spectral region

sigma factor RpoS in *E. coli* [44]. Involvement of epigenetic modulation in antibiotic resistance of bacteria was also studied but by concentrating on certain functions rather than whole profile [45]. We found that Ag exposure changes cytosine methylation profile of DNA in both bacteria, but in an opposite manner: Ag decreased the percentage of cytosine methylated DNA in *E. coli* whereas increased in *S. aureus*. Since DNA sugar puckering is claimed to be affected by cytosine methylation [46, 47], we further identified the relation between DNA cytosine methylation levels and sugar conformation by Pearson correlation. Although Banyay et al described the increased contribution of C2′-endo type of sugar in the methylated sequences, we found a negative correlation between *S*-type conformation and cytosine methylation status of DNA in both bacteria ($r = -.9863$, $P = .0003$ for *E. coli* and $r = -.9757$, $P = .0045$ in *S. aureus*). Since the previous studies performed with model DNA duplex having predetermined short sequence, this contradictory finding may be caused by the use of genomic DNA in this study. Despite this negative correlation, a strong positive correlation between *N*-type conformation (867 cm^{-1} and 883 cm^{-1} bands) and *A*-DNA ($r = .9994$, $P < .0001$ for 867 cm^{-1} band and $r = .9934$, $P < .0001$ for 883 cm^{-1} band in *S. aureus*), and *S*-type conformation and *Z*-DNA were found ($r = 1.000$, $P < .0001$ in *E. coli*). These results suggest that the effect of cytosine methylation on DNA structure overwhelmed by direct (binding to nucleotides) or indirect (DNA damage) effects of Ag on DNA conformation and topology.

4 | CONCLUSION

Ag is a heavy metal having a long history of general use as an antimicrobial agent for prevention and control of infections. However, concerns are being expressed regarding the emergence of bacterial resistance to Ag, especially within the clinical environment [48]. On the other hand, Ag resistance is an important concept for bioremediation technologies to clean Ag-contaminated areas and recycle Ag from waste generated by the industries [36, 49]. Therefore, understanding of the mechanisms and molecular aspects of Ag resistance is important to enhance antimicrobial efficacy and specificity for enhanced therapeutic benefits and for biotechnological applications. Analysis of IR spectra gave us clues on the necessity of extensive molecular alterations for bacterial systems' adaptation to Ag. Changes in DNA molecules can affect gene expression patterns and the resulting effective flexibility of the metabolism makes bacteria superbly adaptive. Our findings proved—otherwise an intuitively deductible phenomenon—that the adaptation of bacteria to high-level metal concentrations in their environment may also be affected by epigenetic modulations. In other words, the adaptation is not the function of few particular changes but it is that of wide-ranging alterations of existing structures and subsequent functional alterations to bring about the physiological response. Therefore, advances in the awareness of epigenetics and their involvement in the development of heavy-metal adaptation in bacteria will be of great significance to understand the mechanisms beyond heavy-metal resistance.

ACKNOWLEDGMENTS

Tübitak (Grant 113Y515) supported this work. The authors thank Dr Sara Banu Akkas for language editing

AUTHOR BIOGRAPHIES

Please see Supporting Information online.

REFERENCES

[1] A. Iyer, K. Mody, B. Jha, *Mar. Pollut. Bull.* **2005**, *50*, 340.

[2] L. Hou, X. Zhang, D. Wang, A. Baccarelli, *Int. J. Epidemiol.* **2012**, *41*, 79.

[3] J. Fabrega, S. N. Luoma, C. R. Tyler, T. S. Galloway, J. R. Lead, *Env. Int.* **2011**, *37*, 517.

[4] D. H. Nies, *FEMS Microbiol. Rev.* **2003**, *27*, 313.

[5] J. A. Lemire, J. J. Harrison, R. J. Turner, *Nat. Rev. Microbiol.* **2013**, *11*, 371.

[6] C. N. Lok, C. M. Ho, R. Chen, P. K. H. Tam, J. F. Chiu, C. M. Che, *J. Proteome Res.* **2008**, *7*, 2351.

[7] A. D. Gupta, S. Karthikeyan, *Ecotoxicol. Env. Saf.* **2016**, *130*, 289.

[8] R. Gurbanov, N. Simsek Ozek, A. G. Gozen, F. Severcan, *Anal. Chem.* **2015**, *87*, 9653.

[9] M. Kardas, A. G. Gozen, F. Severcan, *Aquat. Toxicol.* **2014**, *155*, 15.

[10] A. Bitto, G. Pizzino, N. Irrera, F. Galfo, F. Squadrito, *Curr. Genomics* **2014**, *15*, 464.

[11] D. H. Nies, *Appl. Microbiol. Biotechnol.* **1999**, *51*, 730.

[12] C. Cervantes, A. E. Espino-Saldana, F. Acevedo-Aguilar, I. L. Leon-Rodriguez, M. E. Rivera-Cano, M. Avila-Rodriguez, K. Wrobel-Kaczmarczyk, K. Wrobel-Zasada, J. F. Gutierrez-Corona, J. S. Rodriguez-Zavala, R. Moreno-Sánchez, *Rev. Latinoam. Microbiol.* **2006**, *48*, 203.

[13] L. Wang, B. Mizaikoff, *Anal. Bioanal. Chem.* **2008**, *391*, 1641.

[14] R. Gurbanov, F. Yıldız, *J. Food Health Sci.* **2017**, *3*, 117.

[15] F. Kucuk Baloglu, S. Garip, S. Heise, G. Brockmann, F. Severcan, *Analyst* **2015**, *140*, 2205.

[16] A. Markowicz, T. Płociniczak, Z. Piotrowska-Seget, *Polish J. Environ. Stud.* **2010**, *19*, 957.

[17] A. Kulp, M. J. Kuehn, *Annu. Rev. Microbiol.* **2010**, *64*, 163.

[18] J. C. Lee, *J. Bacteriol. Virol.* **2012**, *42*, 181.

[19] W. Yi, X. Liu, Y. Li, J. Li, C. Xia, G. Zhou, W. Zhang, W. Zhao, X. Chen, P. G. Wang, *Proc. Nat. Acad. Sci. U. S. A.* **2009**, *106*, 4207.

[20] A. S. Kumar, K. Mody, B. Jha, *J. Basic Microbiol.* **2007**, *47*, 103.

[21] A. Jaroslawiecka, Z. Piotrowska-Seget, *Microbiology* **2014**, *160*, 12.

[22] F. Severcan, P. I. Haris, *Vibrational Spectroscopy in Diagnosis and Screening*, IOS Press, Amsterdam, The Netherlands, **2012**.

[23] K. T. Militello, A. H. Mandarano, O. Varechtchouk, R. D. Simon, *FEMS Microbiol. Lett.* **2014**, *350*, 100.

[24] C. Nithya, B. Gnanalakshmi, S. K. Pandian, *Mar. Environ. Res.* **2011**, *71*, 283.

[25] M. Wenning, F. Breitenwieser, R. Konrad, I. Huber, U. Busch, S. Scherer, *J. Microbiol. Methods* **2014**, *103*, 44.

[26] A. A. de Lima e Silva, M. A. Ribeiro de Carvalho, S. A. L. L. de Souza, P. M. Teixeira Dias, R. G. da Silva Filho, C. S. de Meirelles Saramago, C. A. de Melo Bento, E. Hofer, *Brazilian J. Microbiol.* **2012**, *43*, 1620.

[27] S. Murinova, K. Dercova, *Int. J. Microbiol.* **2014**, *2014*, 1. https://doi.org/10.1155/2014/873081.

[28] S. Rottem, *FEBS Lett*. **1978**, *95*, 121.

[29] T. J. Denich, L. A. Beaudette, H. Lee, J. T. Trevors, *J. Microbiol. Methods* **2003**, *52*, 149.

[30] H. J. Heipieper, F. Meinhardt, A. Segura, *FEMS Microbiol. Lett.* **2003**, *229*, 1.

[31] G. Franci, A. Falanga, S. Galdiero, L. Palomba, M. Rai, G. Morelli, M. Galdiero, *Molecules* **2015**, *20*, 8856.

[32] Q. L. Feng, J. Wu, G. Q. Chen, F. Z. Cui, T. N. Kim, J. O. Kim, *J. Biomed. Mater. Res.* **2000**, *52*, 662.

[33] M. T. Madigan, J. M. Martinko, K. S. Bender, D. H. Buckley, D. A. Stahl, *Brock Biology of Microorganisms*, 14th ed., Pearson, Boston, MA **2015**.

[34] H. Arakawa, J. F. Neault, H. A. Tajmir-Riahi, *Biophys. J.* **2001**, *81*, 1580.

[35] H. J. Park, J. Y. Kim, J. Kim, J. H. Lee, J. S. Hahn, M. B. Gu, J. Yoon, *Water Res.* **2009**, *43*, 1027.

[36] T. C. Dakal, A. Kumar, R. S. Majumdar, V. Yadav, *Front. Microbiol.* **2016**, *7*, 1831.

[37] A. D. S. Cameron, D. M. Stoebel, C. J. Dorman, *Mol. Microbiol.* **2011**, *80*, 85.

[38] D. R. Whelan, T. J. Hiscox, J. I. Rood, K. R. Bambery, D. McNaughton, B. R. Wood, *J. R. Soc. Interface* **2014**, *11*, 20140454.

[39] J. Anastassopoulou, *J. Mol. Struct.* **2003**, *651-653*, 19.

[40] B. F. Eichman, G. P. Schroth, B. E. Basham, P. S. Ho, *Nucleic Acids Res.* **1999**, *27*, 543.

[41] J. V. Ditlevson, S. Tornaletti, B. P. Belotserkovskii, V. Teijeiro, G. Wang, K. M. Vasquez, P. C. Hanawalt, *Nucleic Acids Res.* **2008**, *36*, 3163.

[42] D. Fragou, A. Fragou, S. Kouidou, S. Njau, L. Kovatsi, *Toxicol. Mech. Methods* **2011**, *21*, 343.

[43] R. Kumar, A. K. Mukhopadhyay, P. Ghosh, D. N. Rao, *PLoS One* **2012**, *7*, e42303.

[44] C. Kahramanoglou, A. I. Prieto, S. Khedkar, B. Haase, A. Gupta, V. Benes, G. M. Fraser, N. M. Luscombe, A. S. N. Seshasayee, *Nat. Commun.* **2012**, *3*, 886.

[45] S. S. Motta, P. Cluzel, M. Aldana, *PLoS One* **2015**, *10*, e0118464.

[46] M. Banyay, A. Gräslund, *J. Mol. Biol.* **2002**, *324*, 667.

[47] L. Martinez-Fernandez, A. Banyasz, L. Esposito, D. Markovitsi, R. Improta, *Signal Transduct. Target. Ther* **2017**, *2*, 17021.

[48] S. L. Percival, P. G. Bowler, D. Russell, *J. Hosp. Infect.* **2005**, *60*, 1.

[49] G. F. Najmuldeen, A. R. M. Hasbi, E. A. Makky, S. H. Mohd Rasdi, J. B. Al-Dabbagh, *Int. J. Curr. Microbiol. Appl. Sci.* **2014**, *3*, 364.

SUPPORTING INFORMATION

Additional Supporting Information may be found online in the supporting information tab for this article.

FILE S1. Additional infrared spectra, band assignment table and details of the conducted experiments

How to cite this article: Gurbanov R, S. Ozek N, Tunçer S, Severcan F, Gozen AG. Aspects of silver tolerance in bacteria: infrared spectral changes and epigenetic clues. *J. Biophotonics*. 2018;11:e201700252. https://doi.org/10.1002/jbio.201700252